nature neuroscience

Differential control of presynaptic efficacy by postsynaptic N-cadherin and β-catenin

Nathalia Vitureira[1], Mathieu Letellier[1], Ian J White[1] & Yukiko Goda[1,2]

N-cadherin is a homophilic adhesion protein that remains expressed at mature excitatory synapses beyond its developmental role in synapse formation. We investigated the trans-synaptic activity of N-cadherin in regulating synapse function in rodent cultured hippocampal neurons using optical methods and electrophysiology. Interfering with N-cadherin in postsynaptic neurons reduced basal release probability (p_r) at inputs to the neuron, and this trans-synaptic impairment of release accompanied impaired vesicle endocytosis. Moreover, loss of the GluA2 AMPA-type glutamate receptor subunit, which decreased p_r by itself, occluded the interference with postsynaptic N-cadherin. The loss of postsynaptic N-cadherin activity, however, did not affect the compensatory upregulation of p_r induced by chronic activity silencing, whereas postsynaptic β-catenin deletion blocked this presynaptic homeostatic adaptation. Our findings suggest that postsynaptic N-cadherin helps link basal pre- and postsynaptic strengths to control the p_r offset, whereas the p_r gain adjustment requires a distinct trans-synaptic pathway involving β-catenin.

© 2012 Nature America, Inc. All rights reserved.

The formation and morphogenesis of nascent synaptic contacts are assisted by adhesion proteins, including cadherins that mediate Ca^{2+}-dependent homophilic intercellular interactions. Recent studies highlight roles for N-cadherin, the most widely expressed classical cadherin family member in neurons, in regulating dendritic spine morphology and synaptic efficacy beyond its established function in shaping developing synaptic networks. Interfering with N-cadherin-dependent adhesion not only produces fewer synapses[1] but also increases dendritic spines with immature morphology[1–4], reduces synaptic vesicle cluster size and turnover[1,3,4] and impairs synaptic plasticity[5,6]. Furthermore, loss of N-cadherin expression also accompanies spine shrinkage and defects in long-term potentiation[7–9] and in short-term synaptic plasticity[10,11].

Neurotransmitter release probability (p_r) is a key presynaptic determinant of synaptic efficacy, and it is dynamically altered during synaptic plasticity. Moreover, p_r is highly heterogeneous among different synapses, even for those formed onto the same neuron[12–14]. Over the past decades, our understanding of the mechanisms of p_r regulation has significantly advanced, particularly with respect to the contribution of intracellular Ca^{2+} dynamics and Ca^{2+}-binding proteins[15,16]. However, we know very little about how basal p_r is set at individual synapses and about how p_r is homeostatically adjusted according to changes in network activity. Recent studies have suggested that p_r is set retrogradely in a manner compensatory to postsynaptic activity[17,18] and that such regulation is implemented locally at the level of dendritic branches[17]. Although molecular mechanisms of the retrograde control of p_r remain to be delineated, both diffusible molecules[19,20] and synapse adhesion proteins[21,22] have been implicated in this process.

Here we have explored whether N-cadherins, through their homophilic interactions, could directionally control synaptic strength and contribute to the retrograde regulation of p_r. We have previously shown that the postsynaptic N-cadherin/β-catenin complex modulates synaptic AMPA receptor (AMPAR) abundance under basal conditions in a cell-autonomous manner ('in *cis*')[5]. Furthermore, loss of β-catenin in postsynaptic neurons prevents homeostatic synaptic scaling of AMPARs induced by chronic changes in network activity. Here we find that interfering with N-cadherin activity selectively in postsynaptic neurons is sufficient to impair presynaptic strength 'in *trans*', an effect that is occluded by the loss of GluA2. In contrast, the ability of synapses to homeostatically adapt p_r remains unaffected. Notably, postsynaptic N-cadherin and β-catenin are differentially required for regulating presynaptic release in *trans*. Unlike loss of N-cadherin, loss of postsynaptic β-catenin does not affect p_r under basal conditions but prevents homeostatic upregulation of p_r induced by activity silencing. Our findings reveal two molecularly dissociable components of presynaptic strength regulation: one for setting the level of basal presynaptic strength and the other for adjusting the gain.

RESULTS

Postsynaptic N-cadherin affects presynaptic organization

To examine how postsynaptic N-cadherin regulated presynaptic organization and function trans-synaptically, we interfered with N-cadherin activity in isolated neurons and studied the properties of presynaptic inputs formed onto such neurons. We first compared the effects of overexpressing C-terminally GFP-tagged wild-type N-cadherin (WT-NCad), a dominant negative N-cadherin lacking the extracellular cadherin repeats required for effective intercellular adhesion (DN-NCad)[5], and a control GFP vector (**Fig. 1**). Neurons were transfected at 10 days *in vitro* (DIV), after the initial wave of synaptogenesis. The low transfection efficiency (<10 neurons per coverslip) ensured that most presynaptic inputs onto a transfected

[1]Medical Research Council Laboratory for Molecular Cell Biology and Cell Biology Unit, University College London, London, UK. [2]RIKEN Brain Science Institute, Wako, Saitama, Japan. Correspondence should be addressed to Y.G. (goda@brain.riken.jp).

Received 8 August; accepted 2 November; published online 4 December 2011; doi:10.1038/nn.2995

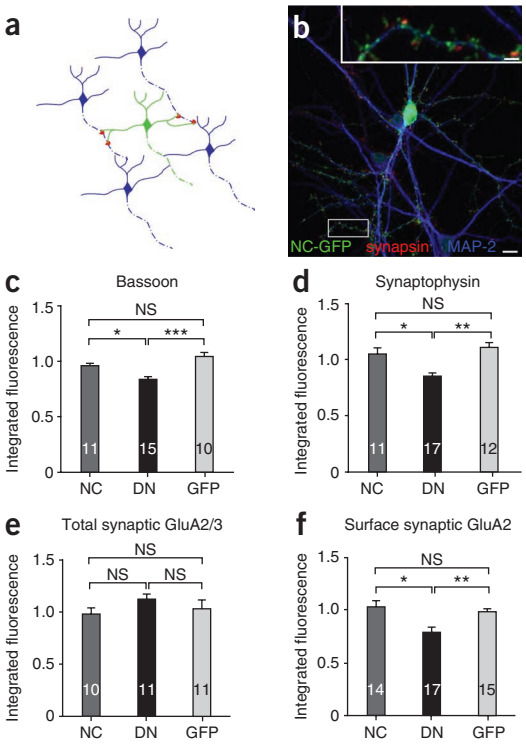

Figure 1 Postsynaptic expression of DN-NCad decreases presynaptic proteins. (**a**) Experimental scheme: owing to a low transfection efficiency, a neuron expressing a construct of interest receives inputs mostly from untransfected cells. Dashed lines, axons; solid lines, dendrites. (**b**) Example image of a hippocampal neuron expressing GFP-tagged WT-NCad and double labeled for synapsin (red) and MAP2 (blue). Boxed area is magnified in inset. Main scale bar, 20 µm; inset, 3 µm. (**c**–**f**) Integrated immunofluorescence intensity of puncta labeled for pre- and postsynaptic proteins in cells postsynaptically expressing WT-NCad (NC), DN-NCad (DN) or GFP. Synaptic puncta were identified by double labeling for bassoon or synaptophysin and GluA2/3 (using a rabbit polyclonal antibody cross-reactive with GluA2 and GluA3), or for synapsin and surface GluA2. Error bars show mean ± s.e.m. for each group relative to untransfected neighboring neurons in the same field of view. The number of neurons is indicated in the bars; $*P < 0.05$, $**P < 0.01$, $***P < 0.001$; NS, no statistically significant difference; one-way analysis of variance (ANOVA) followed by Tukey's test.

neuron originated from untransfected control neurons (**Fig. 1a**,**b**). Consistent with a reported role for N-cadherins in synapse formation and maintenance[1], DN-NCad neurons received ~40% fewer synapses than controls, whereas WT-NCad neurons had a synapse density comparable to that of control neurons (data not shown). To assess whether postsynaptic N-cadherin affected the presynaptic organization trans-synaptically, we quantified synaptophysin, an abundant synaptic vesicle membrane protein, and bassoon, an active zone component, by immunofluorescence labeling (**Fig. 1c**,**d** and **Supplementary Fig. 1**). Compared to synapses on control untransfected neurons, synapses remaining on DN-NCad neurons showed less synaptophysin and bassoon (fold respectively: DN-NCad, 0.85 ± 0.03 and 0.79 ± 0.06; WT-NCad, 1.05 ± 0.05 and 1.03 ± 0.07; GFP, 1.11 ± 0.05 and 0.98 ± 0.03), suggesting that there were fewer synaptic vesicles and a smaller active zone when N-cadherin activity was trans-synaptically impaired. We also determined the cell-autonomous effect of DN-NCad on post-synaptic receptors in *cis*. Live labeling for surface GluA2 AMPAR subunit also revealed a specific reduction in synaptic GluA2 signal (apposed to synapsin I) in DN-NCad (0.78 ± 0.06; $P < 0.01$) but not in WT-NCad neurons (1.03 ± 0.06; $P > 0.2$) relative to controls (0.98 ± 0.03) (**Fig. 1f**), consistent with our previous observations on quantal amplitudes[5]. Total synaptic AMPAR, however, was unchanged for neurons expressing WT-NCad (0.98 ± 0.06; $P > 0.2$), DN-NCad (1.14 ± 0.06; $P > 0.2$) or control GFP (1.02 ± 0.08; $P > 0.2$) compared to untransfected cells on the same coverslip (**Fig. 1e**), suggesting that DN-NCad specifically altered the surface-to-intracellular distribution of AMPARs.

We next investigated the ultrastructural organization of presynaptic boutons on neurons transfected with the N-cadherin constructs by correlative light and serial electron microscopy (**Fig. 2a**,**b**). Synapses had a normal appearance whether they contacted the dendrites of WT-NCad, DN-NCad or control GFP neurons. However, quantification revealed that there were significantly fewer total synaptic vesicles at boutons on DN-NCad neurons than at those on control or WT-NCad neurons (DN-NCad, 132 ± 9 ($P < 0.001$); WT-NCad, 237 ± 14; GFP, 245 ± 12; **Fig. 2c**). Furthermore, the number of vesicles docked at the active zone was also smaller in presynaptic boutons on DN-NCad neurons than on control GFP or WT-NCad neurons (DN-NCad, 3.0 ± 0.4 ($P < 0.001$); WT-NCad, 6.0 ± 0.4; GFP, 7.0 ± 0.6; **Fig. 2d**).

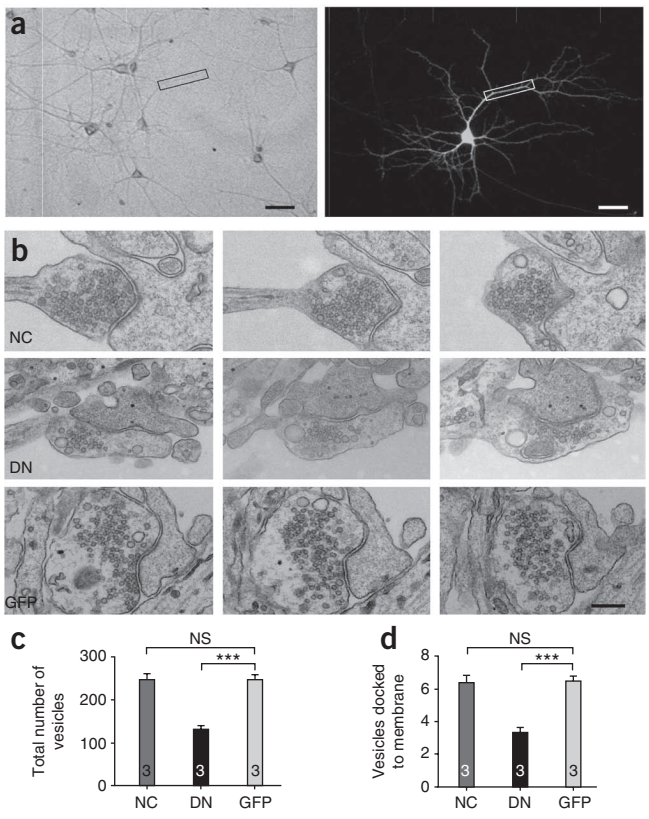

Figure 2 Ultrastructural analysis of synaptic vesicle distribution. (**a**) Brightfield (left) and fluorescence (right) images of a representative transfected hippocampal neuron used for correlative light and electron microscopy analysis. Scale bars, 50 µm. (**b**) Three consecutive serial sections of example synapses formed onto dendrites expressing WT-NCad (NC), DN-NCad (DN) or GFP. Scale bar, 100 nm. (**c**,**d**) Summary of the total number of vesicles (**c**) and the number of vesicles docked to the active zone (**d**). Error bars show mean ± s.e.m. The number of neurons used is shown in the bars; $n = 23$, 16 and 24 synapses for NC, DN and GFP, respectively. One-way ANOVA followed by Tukey's test. $***P < 0.001$; NS, no statistically significant difference.

© 2012 Nature America, Inc. All rights reserved.

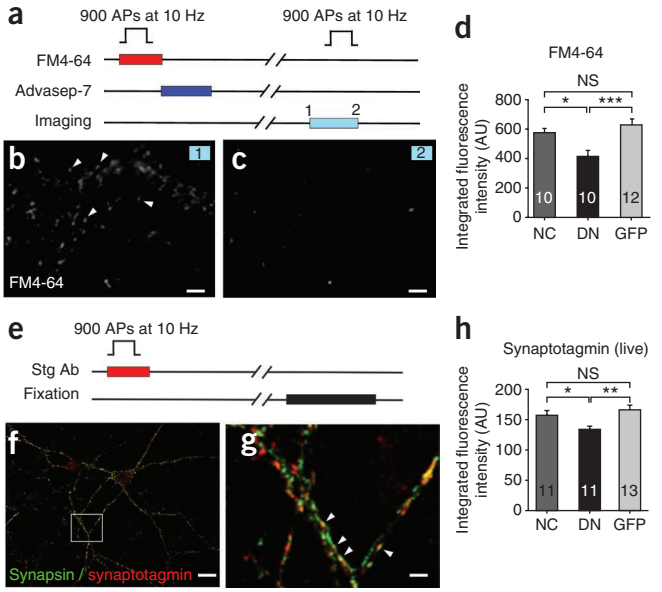

Figure 3 Disrupting postsynaptic N-cadherin activity decreases the size of the recycling synaptic vesicle pool. (**a**) Scheme for FM dye experiments. Advasep-7 is an FM-chelating agent used to help remove excess dye. AP, action potential. (**b**,**c**) Example images of FM4-64 dye-loaded synapses before (**b**) and after (**c**) unloading stimulation. Scale bars, 4 μm. (**d**) Summary of FM4-64 fluorescence intensity of the labeled recycling vesicle pool at single synapses formed onto dendrites expressing WT-NCad (NC), DN-NCad (DN) or GFP. AU, arbitrary units. (**e**) Live labeling protocol using synaptotagmin antibody (Stg Ab) to visualize the recycling vesicles. (**f**) Representative fluorescence image of hippocampal cultures double labeled with synaptotagmin (live; red) and synapsin (after fixation; green). Scale bar, 15 μm. (**g**) Higher magnification of the boxed region in **f**. Arrowheads indicate active boutons where the two presynaptic proteins colocalize. Scale bar, 2 μm. (**h**) Summary of synaptotagmin immunofluorescence intensity representing recycling vesicles at boutons formed onto dendrites expressing NC, DN or GFP. Error bars show mean ± s.e.m. The number of neurons used is shown in the bars. $^{*}P < 0.05$, $^{**}P < 0.01$, $^{***}P < 0.001$; NS, no statistically significant difference; one-way ANOVA followed by Tukey's test.

These observations are consistent with results from immunofluorescence analysis for synaptophysin and bassoon, which were diminished specifically in DN-NCad–expressing neurons. Thus, postsynaptic expression of DN-NCad is sufficient to trans-synaptically compromise the presynaptic organization. Notably, postsynaptic overexpression of WT-NCad had no effects on the presynaptic organization. This could be due to the limited availability of the NCad interacting proteins that are involved in the presynaptic regulation, such that excess postsynaptic NCad on its own is ineffective.

N-cadherin affects presynaptic efficacy in *trans*

To determine whether the presynaptic morphological changes induced by the postsynaptic DN-NCad were associated with functional changes, we monitored synaptic vesicle dynamics using the styryl dye FM4-64 or an antibody to the luminal domain of synaptotagmin I. Field stimulation (900 action potentials at 10 Hz) was applied to neurons in the presence of FM4-64 or the synaptotagmin antibody to label the total recycling pool of synaptic vesicles (**Fig. 3**). The recycling pool was significantly smaller in boutons on DN-NCad neurons but not on WT-NCad neurons relative to those on control neurons (in arbitrary units: for FM dye, DN-NCad 411 ± 45 ($P < 0.001$), WT-NCad 575 ± 29, GFP 629 ± 38; **Fig. 3d**; for synaptotagmin, DN-NCad 124 ± 5 ($P < 0.001$), WT-NCad 150 ± 7, GFP 159 ± 8; **Fig. 3h**). To test whether this smaller recycling pool accompanied a decrease in release probability, we performed optical quantal analysis to estimate p_r at individual synapses[13,23,24] (**Fig. 4a**,**b**). Boutons formed onto DN-NCad neurons showed a 42% lower p_r, whereas no change was observed at WT-NCad neurons, in comparison to GFP or untransfected controls (DN-NCad 0.20 ± 0.01 ($P < 0.001$), WT-NCad 0.33 ± 0.02, GFP 0.35 ± 0.03, untransfected 0.34 ± 0.03).

Intercellular adhesion mediated by classical cadherins is highly dependent on extracellular calcium[25]. We therefore wondered whether the trans-synaptic decrease in p_r caused by the postsynaptic expression of DN-NCad could be linked to the loss of Ca^{2+} sensitivity of neurotransmitter release—for example, by affecting the organization or activity of Ca^{2+} channels. However, raising the extracellular Ca^{2+} from 2 to 5 mM increased p_r at synapses on DN-NCad neurons by ~50% (0.18 ± 0.02 to 0.28 ± 0.02), an extent comparable to the p_r increase observed at control GFP neurons under the same conditions (0.27 ± 0.01 to 0.41 ± 0.02; **Fig. 4c**). Thus, despite the reduced p_r, synapses on DN-NCad neurons retained the capacity to respond to changes in extracellular Ca^{2+}.

As DN-NCad acts as a dominant negative for all classical cadherins, we confirmed the specificity for postsynaptic N-cadherin in regulating p_r using a short hairpin RNA to knock down endogenous N-cadherin in postsynaptic neurons. Presynaptic boutons on neurons expressing the shRNA, whose potency in reducing N-cadherin in hippocampal neurons has been previously confirmed[8], showed a lower p_r (0.15 ± 0.02%) than boutons on neurons receiving a scrambled shRNA (0.23 ± 0.01; $P < 0.01$; **Supplementary Fig. 2**), and the extent of decrease of p_r was comparable to that observed for DN-NCad–expressing neurons (**Fig. 4b**). Therefore, loss of postsynaptic N-cadherin activity is sufficient to compromise neurotransmitter release in *trans*.

We also confirmed the specificity for postsynaptic N-cadherin impairment on presynaptic organization in *trans* and AMPAR levels in *cis* using the shRNA (**Supplementary Fig. 2**). Bassoon, synaptophysin and surface GluA2 immunofluorescence intensity at synapses received by shRNA-expressing neurons were significantly reduced ($P < 0.001$) compared to intensity at synapses received by control scrambled shRNA neurons (fold relative to untransfected neurons: for bassoon, N-cadherin shRNA 0.64 ± 0.06, scrambled 0.98 ± 0.04; for synaptophysin, N-cadherin shRNA 0.70 ± 0.04, scrambled 1.0 ± 0.07; for surface GluA2, N-cadherin shRNA 0.67 ± 0.05, scrambled 1.02 ± 0.07), similarly to the reduction we observed for the DN-NCad overexpression.

The major intracellular binding partner of N-cadherin is β-catenin, which, together with α-catenin, links cadherins to the F-actin cytoskeleton. To test whether β-catenin functions in the trans-synaptic modulation of presynaptic function by N-cadherin, we first examined whether impairing N-cadherin activity altered the localization of β-catenin. The pattern of synaptic distribution of endogenous β-catenin was not appreciably different in DN-NCad neurons compared to WT-NCad or control GFP neurons (**Supplementary Fig. 3**). We next tested whether the ability of postsynaptic N-cadherin to regulate presynaptic release required its interaction with β-catenin by overexpressing a mutant N-cadherin lacking the β-catenin binding region in its C-terminal domain (NC-ΔC)[5]. Synapses formed onto NC-ΔC neurons showed a p_r comparable to control neurons (NC-ΔC, 0.28 ± 0.03; GFP, 0.33 ± 0.02; $P > 0.2$; **Supplementary Fig. 2**), suggesting that postsynaptic N-cadherin modulates presynaptic release in a β-catenin-independent manner.

To further clarify whether β-catenin can regulate p_r in *trans*, we used cultures from mice with a *loxP*-flanked ('floxed') β-catenin gene[26] to knock down endogenous β-catenin by expressing Cre recombinase in

© 2012 Nature America, Inc. All rights reserved.

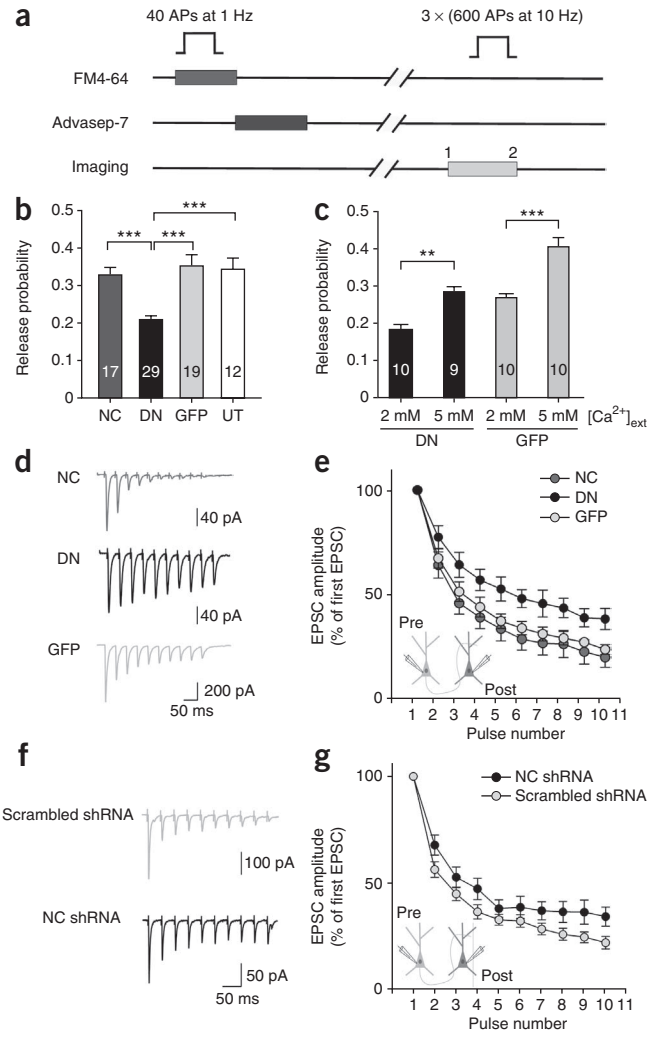

Figure 4 Postsynaptic N-cadherin modulates neurotransmitter release probability. (**a**) Experimental protocol for estimating p_r using the optical quantal analysis. AP, action potential. (**b**) Summary of p_r at single boutons expressing WT-NCad (NC), DN-NCad (DN) or GFP postsynaptically. Untransfected cells (UT) were used as controls. (**c**) Effect of increasing extracellular (ext) [Ca^{2+}] on p_r. Error bars show mean ± s.e.m. The number of neurons used is shown in the bars. $^{**}P < 0.01$, $^{***}P < 0.001$; one-way ANOVA followed by Tukey's test (**b**,**c**). (**d**–**g**) Representative traces of EPSCs elicited by a train of ten action potentials at 25 Hz from connected cell pairs in which the postsynaptic neuron overexpresses NC, DN or GFP (**d**) or NC shRNA or control scrambled shRNA (**f**), and graphs showing averaged EPSC amplitudes recorded in monosynaptically connected postsynaptic neurons (**e**,**g**). Insets depict the recording configuration. Note the smaller depression of EPSC amplitudes for neurons overexpressing the DN compared to NC or GFP neurons (two-tailed Student's *t*-test, $P < 0.05$; $n = 11$, 7 and 10 cell pairs for NC, DN and GFP, respectively) and the NC shRNA compared to neurons receiving control scrambled shRNA (two-tailed Student's *t*-test, $P < 0.05$; $n = 13$ and 15 cell pairs for NC shRNA and scrambled shRNA, respectively). Error bars show mean ± s.e.m.

sparse numbers of neurons, and determined the consequence on presynaptic organization and function as described above (**Supplementary Fig. 4**). Neurons transfected with Cre-IRES-GFP at10 DIV showed a loss of β-catenin immunofluorescence labeling by DIV 14 (ref. 5). In contrast to impairing postsynaptic N-cadherin activity, postsynaptic loss of β-catenin produced no changes in synaptophysin and bassoon abundance compared to control IRES-GFP or untransfected neurons (relative to untransfected neurons: synaptophysin Cre-IRES-GFP 0.96 ± 0.02, IRES-GFP 1.00 ± 0.03, $P > 0.2$; bassoon Cre-IRES-GFP 0.97 ± 0.06, IRES-GFP 0.99 ± 0.04, $P > 0.2$). Likewise, optical quantal analysis revealed no significant differences in p_r in boutons on β-catenin ablated neurons (0.28 ± 0.02) compared to that in boutons on control IRES-GFP neurons (0.25 ± 0.02, $P > 0.2$; **Supplementary Fig. 2f**). Altogether, these results suggest that the trans-synaptic regulation of basal presynaptic strength does not require postsynaptic β-catenin. We also determined the effect of β-catenin loss on the postsynaptic AMPAR abundance in *cis*. Synaptic GluA2 was lower in β-catenin ablated neurons (0.92 ± 0.03 fold) than in control IRES-GFP neurons (1.10 ± 0.04 fold; $P < 0.05$; **Supplementary Fig. 4e**), consistent with our previous finding of a role for β-catenin in regulating synaptic AMPAR currents in *cis*[5].

To confirm our finding of trans-synaptic regulation of neurotransmitter release by postsynaptic N-cadherin in an independent assay, we performed whole-cell patch clamp recordings from connected cell pairs in which the postsynaptic neuron overexpressed WT-NCad, DN-NCad or control GFP, or shRNA for N-cadherin or control scrambled shRNA. Short-term depression is a form of plasticity in which the extent of depression of postsynaptic responses to successive stimulation correlates with the initial p_r, with synapses having higher p_r producing larger depression and those with lower p_r showing smaller depression[16]. We monitored short-term depression by evoking trains of ten action potentials at 25 Hz in the presynaptic neuron and recording excitatory postsynaptic currents (EPSCs) in the monosynaptically connected postsynaptic neuron. Peak EPSC amplitudes depressed significantly less for postsynaptic neurons overexpressing DN-NCad than for those expressing WT-NCad or GFP, and likewise, significantly less for neurons expressing N-cadherin shRNA than for those with control scrambled shRNA (**Fig. 4d**–**g**). This result is consistent with our observations of the reduced p_r of synapses on DN-NCad or N-cadherin knockdown neurons from optical quantal analysis, and it further confirms the role of N-cadherin in regulating basal neurotransmitter release in *trans*.

We also monitored short-term depression from connected cell pairs in which β-catenin in the postsynaptic neuron was knocked down. In agreement with optical quantal analysis, loss of β-catenin had no effect on the rate of depression of EPSC amplitudes (**Supplementary Fig. 4f**). Therefore, unlike postsynaptic N-cadherin, postsynaptic β-catenin is not required in *trans* to regulate basal p_r.

Effectors of presynaptic regulation by N-cadherin in *trans*

Because N-cadherin is a homophilic adhesion protein, postsynaptic N-cadherin could influence presynaptic strength by interacting with presynaptic N-cadherin. In this case, interfering with N-cadherin activity presynaptically should mimic the effects of postsynaptic N-cadherin disruption. Unexpectedly, however, synapses between axons overexpressing WT-NCad, DN-NCad or control GFP (identified by co-labeling for neurofilament H or Tau) and dendrites of untransfected neurons showed similar levels of synaptophysin and bassoon to synapses between untransfected axons and dendrites (synaptophysin and bassoon, respectively: WT-NCad, 1.10 ± 0.09 and 0.98 ± 0.06; DN-NCad, 0.90 ± 0.03 and 0.95 ± 0.06; GFP, 0.98 ± 0.05 and 0.98 ± 0.05; $P > 0.2$; **Fig. 5a**,**b**). Moreover, we found no significant differences in p_r for boutons along axons of WT-NCad or DN-NCad neurons relative to control GFP neurons by optical quantal analysis (WT-NCad, 0.18 ± 0.03; DN-NCad, 0.18 ± 0.03; GFP, 0.24 ± 0.03; $P > 0.2$; **Fig. 5c**). Such a lack of change in presynaptic release was also supported by paired recordings in which short-term depression was

© 2012 Nature America, Inc. All rights reserved.

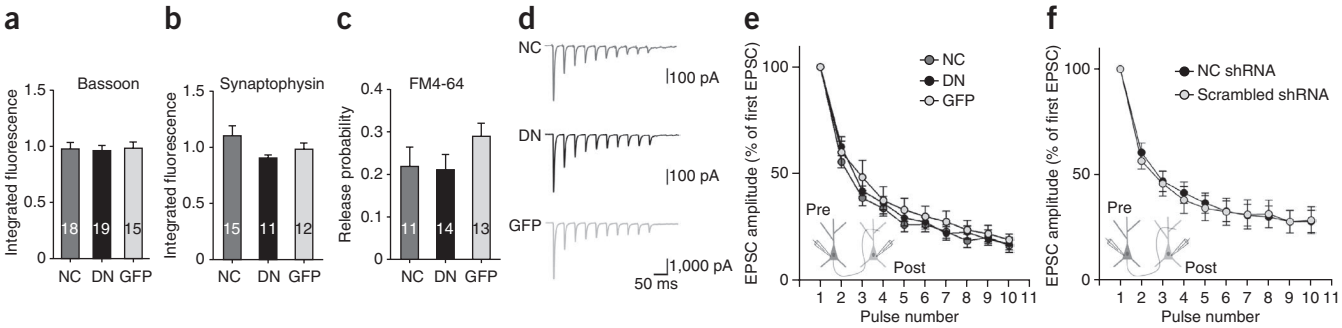

Figure 5 Presynaptic disruption of N-cadherin activity does not affect neurotransmitter release. (**a**,**b**) Summary of bassoon (**a**) and synaptophysin (**b**) puncta intensity along axons expressing WT-NCad (NC), DN-NCad (DN) or GFP. Cells were double labeled for bassoon and neurofilament H or for synaptophysin and Tau. (**c**) Summary of p_r at single boutons expressing NC, DN or GFP presynaptically. The number of neurons is shown in the bars. Data are mean ± s.e.m.; one-way ANOVA followed by Tukey's test; $P > 0.1$. (**d**) Representative traces of EPSC recordings elicited by a ten-action-potential, 25-Hz pulse train from connected cell pairs in which the presynaptic neuron overexpresses NC, DN or control GFP. (**e**,**f**) Graphs showing averaged EPSC amplitudes recorded in monosynaptically connected cell pairs in which presynaptic neurons express NC ($n = 11$), DN ($n = 7$) or GFP ($n = 10$) (**e**) and NC shRNA ($n = 13$) or scrambled shRNA ($n = 15$) (**f**); two-tailed Student's *t*-test, $P > 0.05$. Error bars show mean ± s.e.m.

© 2012 Nature America, Inc. All rights reserved.

similar whether the presynaptic neuron overexpressed WT-NCad, DN-NCad or control GFP or was knocked down for N-cadherin or expressed control scrambled shRNA (**Fig. 5d–f**). Thus, interfering with presynaptic N-cadherin was not sufficient to impair neurotransmitter release in *cis*, in contrast to the potent effect of impairing postsynaptic N-cadherin in *trans*. Furthermore, a lack of effect of presynaptically disrupting N-cadherin activity suggests that postsynaptic N-cadherin adjusts presynaptic strength retrogradely by mechanisms that function independently of presynaptic N-cadherin.

Previous studies have implicated N-cadherin and GluA2 AMPAR subunits in regulating synaptic integrity and function[27,28]; moreover, these two proteins may interact directly to effect their control[9]. We therefore addressed the question of GluA2 in the N-cadherin-dependent trans-synaptic regulation of release by impairing postsynaptic N-cadherin activity when GluA2 expression was knocked down by short interfering RNA (**Fig. 6**). Loss of GluA2 by itself without manipulating N-cadherin activity was sufficient to reduce p_r (scrambled siRNA and GFP control, 0.29 ± 0.02; GluA2 siRNA and GFP control, 0.18 ± 0.02; $P < 0.001$). Moreover, in the absence of GluA2, overexpressing either WT-NCad or DN-NCad had no extra effect on p_r compared to overexpressing control GFP (GluA2 siRNA and DN-NCad, 0.18 ± 0.01; GluA2 siRNA and WT-NCad, 0.16 ± 0.01; $P > 0.2$). Cell pair recordings in which the postsynaptic neuron was knocked down for GluA2 also showed slower short-term depression than control neurons, in line with the decreased p_r (**Fig. 6d**). Furthermore, in GluA2 knockdown neurons, overexpressing DN-NCad did not further reduce the rate of synaptic depression compared to overexpressing WT-NCad or control GFP, suggesting a lack of further change in p_r upon loss of GluA2. Collectively, both optical quantal analysis and patch clamp recordings indicate that loss of GluA2 occludes the effect of impairing N-cadherin activity on p_r, and thus GluA2 could mediate the trans-synaptic actions of N-cadherin.

Neuroligin 1 (NLG-1) is another possible interactor of N-cadherin that might mediate its presynaptic regulation. A recent study reported a cooperative role for NLG-1 in controlling synaptic vesicle accumulation at developing synapses[11]. To test for potential involvement for NLG-1 in the N-cadherin-dependent trans-synaptic presynaptic

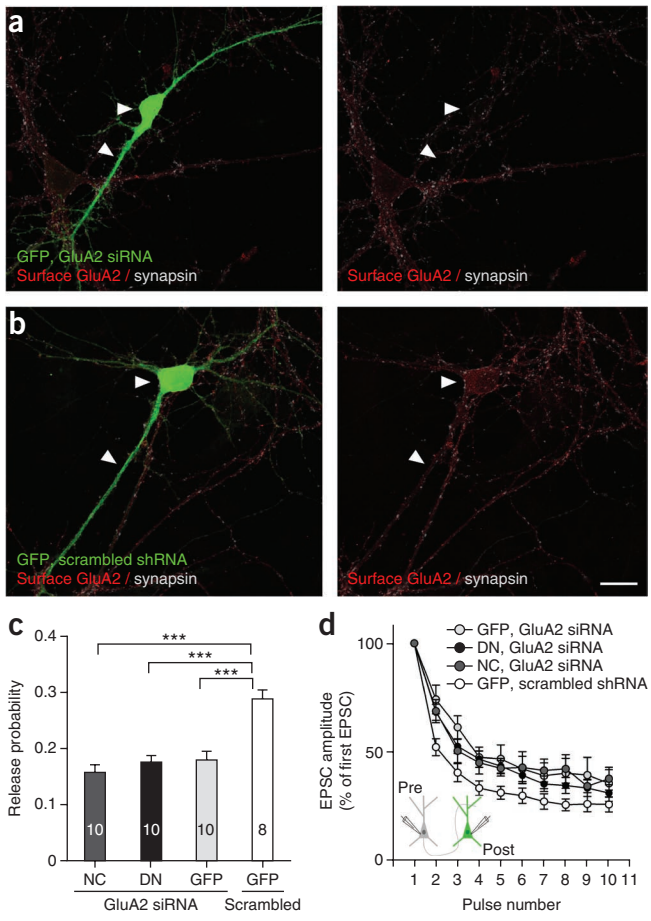

Figure 6 GluA2 is a possible effector of the trans-synaptic regulation of release by N-cadherin. (**a**,**b**) Hippocampal cultures expressing GluA2 siRNA (green) (**a**) show lower surface GluA2 (red) than cells expressing control scrambled siRNA (**b**); arrowheads indicate the soma and a prominent dendrite of the transfected neuron to help align left and right panels. Scale bar, 20 µm. (**c**) Summary of p_r at single boutons co-expressing WT-NCad (NC), DN-NCad (DN) or GFP and GluA2 siRNA, or co-expressing GFP and scrambled control. Error bars show mean ± s.e.m. The number of neurons used is shown in the bars. ***$P < 0.001$; one-way ANOVA followed by Tukey's test. (**d**) Graph showing averaged EPSC amplitudes recorded in monosynaptically connected postsynaptic neurons. Note the smaller depression of EPSC amplitudes for neurons co-expressing NC ($n = 7$), DN ($n = 11$) or GFP ($n = 9$) and the GluA2 siRNA compared to control cells co-expressing GFP and scrambled siRNA ($n = 12$). Two-tailed Student's *t*-test, $P < 0.05$. Inset illustrates the recording configuration. Error bars show mean ± s.e.m.

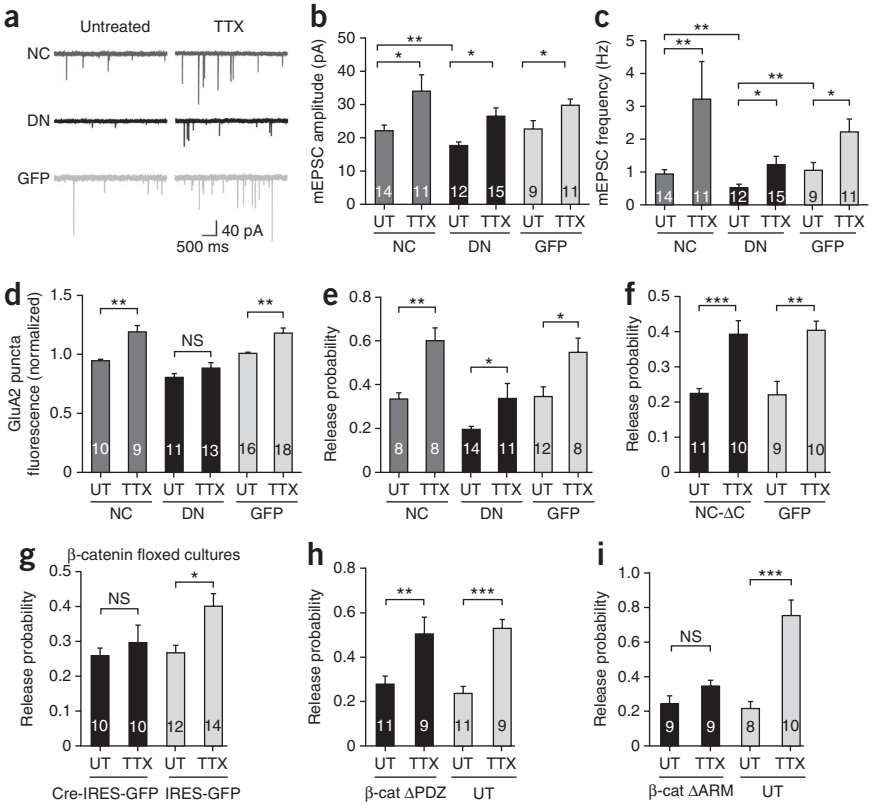

Figure 7 N-cadherin and β-catenin are differentially required for homeostatic regulation of release probability. (**a**–**c**) Effects of chronically blocking network activity with TTX on mEPSC recordings from neurons expressing WT-NCad (NC), DN-NCad (DN) or GFP. Representative traces of mEPSC recordings for each condition (**a**). Summary of mean mEPSC amplitude (**b**) and frequency (**c**), comparing untreated (UT) and TTX-treated groups for NC, DN or GFP neurons. Two-tailed Student's *t*-test or, when criteria for normality were not met, Mann-Whitney test; $*P < 0.05$, $**P < 0.01$. (**d**) Summary of homeostatic scaling of postsynaptic GluA2. The plot shows integrated fluorescence intensity of surface synaptic GluA2 puncta apposed to synapsin labeling in cells postsynaptically expressing NC, DN or GFP. Data are expressed as mean ± s.e.m. relative to control untransfected neurons not treated with TTX. (**e**–**i**) Effects of chronic activity blockade on homeostatic increase in release probability as determined by optical quantal analysis in wild-type cultures of cells expressing NC, DN or GFP (**e**), NC-ΔC or GFP (**f**), and β-cat ΔPDZ (**h**) or β-cat ΔARM (**i**) compared to neighboring untransfected cells, and in β-catenin floxed hippocampal neurons transfected with Cre-IRES-GFP or control IRES-GFP (**g**). Error bars show mean ± s.e.m. $*P < 0.05$, $**P < 0.01$, $***P < 0.001$; NS, no statistically significant difference; one-way ANOVA followed by Tukey's test. The number of neurons used for each group is shown in the bars.

modulation, we examined whether impairing postsynaptic N-cadherin altered its synaptic localization. Double immunofluorescence labeling for neuroligin (using a pan-neuroligin antibody) and vesicular glutamate transporter (VGlut) to identify excitatory synapses where NLG-1 is enriched[29] showed that the synaptic abundance of neuroligin was not significantly different in neurons overexpressing DN-NCad (402 ± 16 arbitrary units (AU)) or WT-NCad (426 ± 36 AU) from that in GFP control (410 ± 27 AU; $P > 0.2$; **Supplementary Fig. 5**). A lack of change in the synaptic localization of neuroligin upon perturbing N-cadherin activity is reminiscent of the lack of change we observed for β-catenin localization in DN-NCad–expressing neurons, and this finding is in agreement with the suggestion that NLG-1 could be linked to the N-cadherin/β-catenin complex by interacting with the β-catenin-binding protein S-SCAM[11]. Therefore, collectively, these observations are consistent with differential functions of postsynaptic N-cadherin and β-catenin in regulating presynaptic function. Moreover, because the cooperative facilitatory action of N-cadherin and NLG-1 in clustering of synaptic vesicles is limited to nascent immature synapses[11], the N-cadherin–dependent mechanism we observe here could arise following a developmental switch in the trans-synaptic control of presynaptic organization.

Postsynaptic N-cadherin and homeostatic plasticity

Homeostatic mechanisms adjust synaptic strength to compensate for changes in network activity and are thought to help maintain neuronal excitation in physiological range[30–32]. Given that interfering with postsynaptic N-cadherin activity was sufficient to impair basal pre- and postsynaptic strengths, we wondered whether in these synapses homeostatic synaptic plasticity might also be compromised. We thus examined the requirement for postsynaptic N-cadherin activity in the compensatory increase in miniature EPSC (mEPSC) amplitude and frequency that are induced by chronically silencing activity with the Na^+ channel blocker TTX[33–36] (**Fig. 7a–c**). In agreement with previous observations, overexpressing DN-NCad in postsynaptic neurons without TTX treatment decreased mean mEPSC amplitude compared to that in control GFP neurons, whereas overexpressing WT-NCad had no effect (DN-NCad ($P < 0.01$), 18 ± 1.1 pA; WT-NCad, 22 ± 1.7 pA; GFP, 23 ± 2.5 pA)[5]. The mean mEPSC frequency was also significantly lower in DN-NCad neurons (DN-NCad, 0.50 ± 0.11 Hz ($P < 0.01$); WT-NCad, 0.91 ± 0.14 Hz; GFP, 1.03 ± 0.24 Hz), consistent with the reduced synaptic density and p_r (see above). TTX treatment (1 μM for 36 h) effectively elicited homeostatic synaptic plasticity in control GFP neurons as confirmed by increased mean mEPSC amplitude (from 23 ± 2.5 to 30 ± 2.0 pA; $P < 0.05$) and frequency (from 1.03 ± 0.24 to 2.20 ± 0.40 Hz; $P < 0.05$) (**Fig. 7a–c** and **Supplementary Fig. 6a**,**b**). Similarly, in neurons overexpressing WT-NCad or DN-NCad, TTX treatment also increased mEPSC amplitude (DN-NCad, from 18 ± 1.1 to 26 ± 2.7 pA; WT-NCad, from 22 ± 1.7 to 34 ± 4.9 pA; $P < 0.05$) and frequency (DN-NCad, from 0.50 ± 0.11 to 1.2 ± 0.25 Hz; WT-NCad, from 0.91 ± 0.14 to 3.2 ± 1.1 Hz; $P < 0.05$) to extents comparable to the changes observed in control GFP neurons. Collectively, interfering with postsynaptic N-cadherin activity does not seem to compromise the ability of synapses to homeostatically adapt their basal pre- and postsynaptic strengths upon chronic activity blockade.

AMPAR trafficking is important in various forms of synaptic plasticity[32,37–39], and synaptic accumulation of AMPA receptors containing GluA1 (refs. 40,41) and/or GluA2 subunits[42–44] could underlie homeostatic scaling of quantal size. Given that N-cadherin interacts with and regulates the trafficking of GluA2-containing AMPARs[9] (although see ref. 45), disrupting postsynaptic N-cadherin activity could alter the subunit composition of synaptic AMPARs. To gain insight into possible differential contribution of GluA1 and GluA2 AMPARs to synaptic scaling in neurons compromised for N-cadherin activity, we compared the average mEPSC waveform between TTX-treated and

© 2012 Nature America, Inc. All rights reserved.

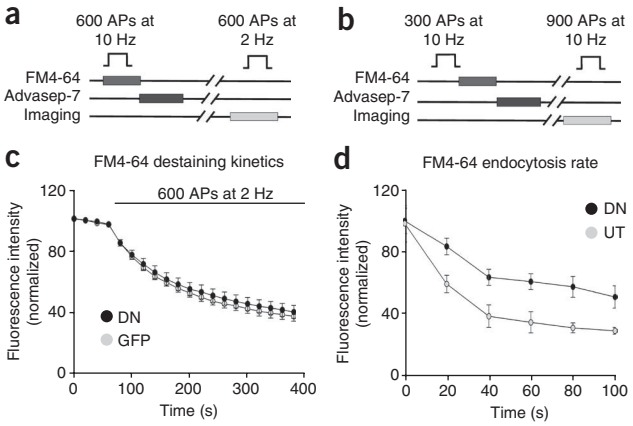

Figure 8 Disrupting postsynaptic N-cadherin activity affects synaptic vesicle endocytosis. (**a**,**b**) Experimental scheme for analyzing the kinetics of exocytosis (**a**) and endocytosis (**b**). The time course of endocytosis is measured by applying the FM dye at a variable time interval (Δt) after the end of stimulation to assess the extent of dye taken up at each time interval. AP, action potential. (**c**) Release kinetics as measured by the time course of FM4-64 destaining during 2-Hz stimulation of 600 action potentials ($n = 107$ boutons for control GFP, $n = 140$ for DN-NCad (DN)). (**d**) Time course of endocytosis at boutons on dendrites of neurons expressing DN or on those of neighboring untransfected (UT) neurons in the same field of view. Each data point was averaged from measurements of individual boutons (DN, $n = 1{,}085$; UT, $n = 1{,}187$) from 4–14 cells in three experiments.

untreated groups for WT-NCad, DN-NCad and control GFP neurons. Although no changes in mEPSC waveform were detected for any group under basal conditions (90–37% decay time: WT-NCad, 4.15 ± 0.23 ms; DN-NCad, 4.40 ± 0.25 ms; GFP, 4.76 ± 0.27 ms; $P > 0.2$), DN-NCad neurons selectively showed a faster mEPSC decay than non-drug-treated cells upon TTX treatment (3.68 ± 0.19 ms; $P < 0.05$); we observed no changes in mEPSC decay for WT-NCad or control GFP neurons upon TTX treatment (WT-NCad, 4.15 ± 0.37 ms; GFP, 4.37 ± 0.33 ms; $P > 0.2$) (**Supplementary Fig. 6c**). The faster decay of mEPSCs in TTX-treated DN-NCad neurons might represent changes in synaptic structure and/or organization associated with impaired postsynaptic N-cadherin activity during homeostatic synaptic plasticity. Alternatively, AMPAR subunit composition might have changed toward GluA1 dominance, as GluA1 currents are larger and decay faster than GluA2 currents[41,46]. In such a case, the scaling up of GluA2 AMPARs after TTX treatment could be compromised in DN-NCad neurons, despite the apparent lack of change in mEPSC amplitude.

To further clarify how N-cadherin might influence the relative contribution of GluA1 and GluA2 to synaptic scaling, we directly monitored surface synaptic GluA1 and GluA2 by live immunolabeling followed by synapsin I labeling to help identify synapses. Whereas TTX treatment increased surface synaptic GluA2 in WT-NCad (from 0.9 ± 0.02 to 1.2 ± 0.05 fold) and control GFP neurons (1.0 ± 0.02 to 1.2 ± 0.04 fold), we detected no such increase in surface synaptic GluA2 in DN-NCad cells upon TTX treatment (from 0.8 ± 0.03 to 0.9 ± 0.05 fold; **Fig. 7d**). Conversely, surface synaptic GluA1 increased in all three conditions after TTX treatment (WT-NCad, from 1.1 ± 0.04 to 1.3 ± 0.05; DN-NCad, from 0.9 ± 0.06 to 1.2 ± 0.04; GFP, from 1.0 ± 0.06 to 1.3 ± 0.07; **Supplementary Fig. 6d**). Taking these results together, DN-NCad specifically altered the subunit composition of synaptic AMPARs during homeostatic synaptic scaling, and postsynaptic N-cadherin function was required for scaling up GluA2 but not GluA1.

The mEPSC frequency is a parameter whose changes could indicate altered p_r, although other factors such as synapse density and postsynaptic silencing could also contribute. Therefore, to corroborate the mEPSC frequency analysis in investigating postsynaptic N-cadherin's role in homeostatic adaptation of presynaptic release, we used optical quantal analysis to estimate p_r and compared the effect of TTX treatment at synapses received by neurons overexpressing WT-NCad, DN-NCad or control GFP (**Fig. 7e**). At boutons on control GFP neurons, TTX significantly increased p_r relative to non-drug-treated cells (from 0.34 ± 0.04 to 0.54 ± 0.05; $P < 0.05$). TTX treatment also increased p_r at synapses on WT-NCad (from 0.33 ± 0.03 to 0.60 ± 0.05; $P < 0.01$) and DN-NCad neurons (from 0.19 ± 0.01 to 0.34 ± 0.07; $P < 0.05$), to an extent comparable to the p_r increase observed in control GFP neurons. Moreover, neurons overexpressing the NC-ΔC mutant, lacking the β-catenin binding region, also showed a similar increase in p_r relative to control GFP neurons upon TTX treatment (from 0.22 ± 0.0.1 to 0.39 ± 0.04 ($P < 0.001$) and from 0.22 ± 0.04 to 0.40 ± 0.03 ($P < 0.01$) for NC-ΔC and control GFP, respectively; **Fig. 7f**). Postsynaptic N-cadherin activity, including its interaction to β-catenin, is therefore not required for the homeostatic upregulation of p_r induced by chronic activity block.

β-catenin in homeostatic regulation of release probability

Our experiments show that, contrary to expectations, postsynaptic N-cadherin and β-catenin have differential effects on presynaptic efficacy and organization in *trans*: unlike impairing postsynaptic N-cadherin activity, ablating postsynaptic β-catenin did not affect the basal p_r and the levels of synaptophysin and bassoon. As the NC-ΔC mutant unable to interact with β-catenin did not block TTX-dependent increase in p_r, we wondered whether homeostatic upregulation of presynaptic strength could also differentially involve postsynaptic N-cadherin and β-catenin in *trans*. We therefore analyzed p_r with or without TTX treatment at synapses where β-catenin was knocked down specifically in postsynaptic neurons using cultures from β-catenin floxed mice (see above). Whereas in control GFP neurons TTX treatment significantly increased p_r relative to non-TTX-treated cells (from 0.25 ± 0.02 to 0.39 ± 0.04; $P < 0.05$), boutons on Cre-IRES-GFP neurons did not upregulate p_r relative to untreated cells (from 0.28 ± 0.02 to 0.26 ± 0.04; $P > 0.2$; **Fig. 7g**). We also carried out pairwise patch clamp recordings in β-catenin floxed cultures where the postsynaptic neuron expressed either Cre or control GFP. TTX treatment increased the rate of synaptic depression to repetitive stimulation only in control GFP and not in β-catenin knockdown neurons expressing Cre (**Supplementary Fig. 4f**), in agreement with a block of upregulation of p_r upon loss of postsynaptic β-catenin. Therefore, postsynaptic β-catenin is required in *trans* for the homeostatic upregulation of p_r induced by chronic activity silencing, whereas postsynaptic N-cadherin activity is dispensable under parallel conditions.

β-catenin has several protein interaction domains. In particular, the central armadillo repeat region mediates binding to N-cadherin and to TCF/LEF transcription factors, while the PDZ binding motif in the C-terminal domain interacts with PDZ adaptor domain–containing proteins such as S-SCAM[11]. To determine whether these two regions function in β-catenin-dependent homeostatic adaptation of presynaptic release, we tested the effect of overexpressing β-catenin deletion mutants lacking the armadillo repeat region (ΔARM) or the PDZ binding motif (ΔPDZ)[5] on p_r by optical quantal analysis with or without TTX treatment (**Fig. 7h**,**i**). As expected from the lack of effect of postsynaptic β-catenin knockdown on basal p_r, we found no difference in p_r between control neurons and neurons overexpressing either β-catenin ΔPDZ or ΔARM mutant under basal conditions. After TTX treatment, however, whereas β-catenin ΔPDZ neurons increased p_r (from 0.28 ± 0.04 to 0.50 ± 0.08; $P < 0.01$) similarly to control neurons (from 0.23 ± 0.03 to 0.53 ± 0.04; $P < 0.001$), we observed no such

© 2012 Nature America, Inc. All rights reserved.

increase for β-catenin ΔARM neurons (0.27 ± 0.04 to 0.34 ± 0.03). Therefore, β-catenin interactions by means of the armadillo repeat region but not the PDZ binding domain are important for presynaptic homeostatic adaptation. Because the association between β-catenin and N-cadherin was dispensable for upregulating p_r upon activity silencing (**Fig. 7f**), transcriptional regulation by β-catenin in postsynaptic neurons is likely to be a key component of the mechanism of retrograde homeostatic modulation.

Postsynaptic N-cadherin affects endocytosis in *trans*

Our finding that the loss of postsynaptic N-cadherin activity compromises p_r in *trans* was based on the optical quantal analysis, which relied on exo-endocytic coupling of synaptic vesicles to monitor the FM dye uptake. Thus, the observed reduction in presynaptic efficacy could be due to alterations in synaptic vesicle exocytosis, endocytosis or both. To clarify this point, we examined the time course of exocytosis and endocytosis separately at boutons on neurons overexpressing DN-NCad or control GFP (**Fig. 8**). First, we analyzed exocytosis by preloading the entire recycling pool with FM4-64 and then monitoring dye destaining kinetics during 2-Hz stimulation (**Fig. 8a**,**c**). Single exponential fits showed no differences in the rate of fluorescent dye loss between synapses expressing the DN-NCad or GFP postsynaptically ($P > 0.2$; decay time constants 108 ± 2.6 s and 113 ± 3.4 s for control and DN-NCad, respectively). Therefore, postsynaptic DN-NCad is not sufficient to trans-synaptically compromise synaptic vesicle exocytosis *per se*.

Next we measured the kinetics of endocytosis by determining the amount of FM dye uptake at different time intervals (Δt) after the end of a 300–action potential stimulus train (**Fig. 8b**,**d**). In this assay, progressively fewer endocytic events are caught with increasing Δt, thereby leading to less dye incorporation into synaptic vesicles, and the rate of reduction in the amount of dye uptake is a measure of the endocytosis rate[47]. Boutons on DN-NCad neurons showed a substantially slower decline in FM dye uptake than control boutons, with half-maximal uptake occurring at about 32 s from the end of stimulation for DN-NCad–expressing neurons and about 18 s for control boutons. Therefore, interfering with postsynaptic N-cadherin activity induced a twofold reduction in the endocytosis rate. These data indicate that postsynaptic N-cadherin controls presynaptic efficacy trans-synaptically by targeting synaptic vesicle endocytosis.

DISCUSSION

We have systematically studied the trans-synaptic regulation of presynaptic efficacy by N-cadherin. Two independent assays for monitoring synaptic vesicle dynamics, FM dyes and antibody to the synaptotagmin I luminal domain, confirmed that interfering with postsynaptic N-cadherin activity reduces transmitter release in *trans,* which was also supported by slowed short-term synaptic depression. Recently, pHluorin-tagged vesicle proteins have been popularly used to monitor synaptic vesicle recycling, particularly in cultured neurons where one can follow single quantal events. We did not use genetically encoded vesicle probes, however, because of the very low yield of synapses that presynaptically express the optical probe and are postsynaptically manipulated for N-cadherin or β-catenin expression.

In contrast to overexpressing DN-NCad or knocking down endogenous N-cadherin, overexpressing WT-NCad in postsynaptic neurons produced no evident changes in the presynaptic organization and release in *trans*. The cytoplasmic domain of N-cadherin interacts with a variety of proteins, such as β-catenin and p120-catenin family members[48]. If the presynaptic modulation by postsynaptic N-cadherin is facilitated or occurs through N-cadherin-interacting proteins, then the abundance and/or activity of the interacting proteins could be limiting, and excess postsynaptic N-cadherin without a binding partner might be ineffective in exerting trans-synaptic control. Notably, overexpressing DN-NCad or WT-NCad or knocking down endogenous N-cadherin in axons has no effect on presynaptic synaptophysin and bassoon levels or on p_r. Therefore, presynaptic N-cadherin seems to be dispensable for controlling the presynaptic organization and function, further highlighting the importance of postsynaptic N-cadherin-interacting proteins for mediating the presynaptic changes.

Our study reveals GluA2 as a potential N-cadherin interactor in the trans-synaptic mechanism that controls p_r. This is in agreement with previous reports of a role for GluA2 in regulating synapse integrity and function[27,28], which may involve a direct interaction between N-cadherin and GluA2 (ref. 9). However, despite the apparent requirement for GluA2 in regulating p_r, the decreased synaptic GluA2 observed with impairment of postsynaptic N-cadherin activity or β-catenin accompanied a reduced p_r only with N-cadherin interference but not with β-catenin loss. Such a lack of change in p_r in β-catenin knockdown neurons could reflect the difference in the way in which GluA2 is reduced when β-catenin is knocked down compared to when N-cadherin activity is impaired. That is, the remaining GluA2 receptors in β-catenin knockdown neurons might still be complexed to and/or interacting with N-cadherin in sufficient numbers to enable presynaptic control.

The reduced p_r upon impairment of postsynaptic N-cadherin activity is associated with a prominent slowing of endocytosis without an appreciable change in exocytosis. The slowed endocytosis could at least partly account for the observed decreases in the total synaptic vesicle number and the recycling vesicle pool size. How might postsynaptic N-cadherin affect presynaptic endocytosis in *trans*? As one possibility, postsynaptic N-cadherin interactors could generate a diffusible retrograde signal or modify other adhesion protein–dependent signaling system spanning the synaptic cleft[49] to target the endocytosis machinery. Alternatively, the endocytosis defect could represent a secondary consequence of some synaptic structural change, for example, implemented by N-cadherin interaction with other adhesion systems[11,22]. Whereas the unaltered mEPSC waveform upon DN-NCad overexpression suggests a lack of change in synaptic cleft geometry[46], impaired postsynaptic N-cadherin activity could subtly introduce mechanical changes to the presynaptic membrane and influence exo-endocytic coupling so as to substantially compromise endocytosis. Moreover, our data do not rule out a potential effect on exocytosis that may have been too small to be detected by the FM dye destaining experiments. In dual patch clamp recordings, the reduced synaptic depression in DN-NCad neurons relative to controls is detectable within 80 ms (**Fig. 4e**); this is much faster than the time scale of endocytosis, which occurs in seconds. Further studies are needed to clarify the mechanism by which a synaptic vesicle endocytosis defect arises when postsynaptic N-cadherin activity is impaired.

We find that postsynaptic N-cadherin and β-catenin differentially affect presynaptic efficacy in *trans*. Whereas postsynaptic N-cadherin is required for basal p_r regulation but not for homeostatic presynaptic adaptation, postsynaptic β-catenin is apparently not required for controlling the basal p_r but is needed for the homeostatic resetting of p_r. Such differential requirements were unexpected given the robust link between N-cadherin and β-catenin[48]. Nevertheless, our findings are in line with a suggestion that excitatory synapses contain a pool of N-cadherin that does not colocalize with β-catenin and responds to synaptic activity in a β-catenin–independent manner[50]. Notably, the differential effects of interfering with postsynaptic N-cadherin and β-catenin also extend to synapse density along dendrites. Postsynaptic DN-NCad overexpression reduces synapse density[1] and mEPSC frequency (**Fig. 7c**), in agreement with a role for postsynaptic

© 2012 Nature America, Inc. All rights reserved.

N-cadherin in synapse formation or stabilization. In contrast, ablating β-catenin in postsynaptic neurons does not alter synapse density or mEPSC frequency[5]. On the basis of the requirements for N-cadherin in setting the basal p_r and, in parallel, for synapse formation or maintenance, it is tempting to speculate that the basal p_r associated with a given synapse is set at the time of synapse formation and may be inherent in the manner in which synapses are formed and maintained. In contrast, the homeostatic adjustment of the gain of p_r, which is dependent on β-catenin and possibly transcriptional modulation, is uncoupled from regulation of synapse stability, thereby allowing an extra level of control. The molecular mechanism by which postsynaptic β-catenin adjusts the presynaptic p_r retrogradely according to the level of network activity will be the aim of future work.

METHODS

Methods and any associated references are available in the online version of the paper at http://www.nature.com/natureneuroscience/.

Note: Supplementary information is available on the Nature Neuroscience website.

ACKNOWLEDGMENTS

We thank R. Kemler (Max Planck Institute of Immunology) for β-catenin floxed mice, T. Okuda (Keio University) and M. Passafaro (University of Milan) for sharing plasmids, D. Elliott for expert technical assistance and the members of the Goda laboratory for discussions. This work was supported by the UK Medical Research Council, the European Union 7th Framework Program EUROSPIN project and the RIKEN Brain Science Institute.

AUTHOR CONTRIBUTIONS

N.V. performed all of the experimental work. M.L. contributed electrophysiology experiments and discussion, and I.J.W. performed electron microscopy. N.V. and Y.G. designed the project and wrote the manuscript.

COMPETING FINANCIAL INTERESTS

The authors declare no competing financial interests.

Published online at http://www.nature.com/natureneuroscience/.
Reprints and permissions information is available online at http://www.nature.com/reprints/index.html.

1. Togashi, H. *et al.* Interneurite affinity is regulated by heterophilic nectin interactions in concert with the cadherin machinery. *J. Cell Biol.* **174**, 141–151 (2006).
2. Abe, K., Chisaka, O., Van Roy, F. & Takeichi, M. Stability of dendritic spines and synaptic contacts is controlled by alpha N-catenin. *Nat. Neurosci.* **7**, 357–363 (2004).
3. Bamji, S.X. *et al.* Role of beta-catenin in synaptic vesicle localization and presynaptic assembly. *Neuron* **40**, 719–731 (2003).
4. Murase, S., Mosser, E. & Schuman, E.M. Depolarization drives beta-Catenin into neuronal spines promoting changes in synaptic structure and function. *Neuron* **35**, 91–105 (2002).
5. Okuda, T., Yu, L.M., Cingolani, L.A., Kemler, R. & Goda, Y. beta-Catenin regulates excitatory postsynaptic strength at hippocampal synapses. *Proc. Natl. Acad. Sci. USA* **104**, 13479–13484 (2007).
6. Tang, L., Hung, C.P. & Schuman, E.M. A role for the cadherin family of cell adhesion molecules in hippocampal long-term potentiation. *Neuron* **20**, 1165–1175 (1998).
7. Bozdagi, O. *et al.* Persistence of coordinated long-term potentiation and dendritic spine enlargement at mature hippocampal CA1 synapses requires N-cadherin. *J. Neurosci.* **30**, 9984–9989 (2010).
8. Mendez, P., De Roo, M., Poglia, L., Klauser, P. & Muller, D. N-cadherin mediates plasticity-induced long-term spine stabilization. *J. Cell Biol.* **189**, 589–600 (2010).
9. Saglietti, L. *et al.* Extracellular interactions between GluR2 and N-cadherin in spine regulation. *Neuron* **54**, 461–477 (2007).
10. Jüngling, K. *et al.* N-cadherin transsynaptically regulates short-term plasticity at glutamatergic synapses in embryonic stem cell-derived neurons. *J. Neurosci.* **26**, 6968–6978 (2006).
11. Stan, A. *et al.* Essential cooperation of N-cadherin and neuroligin-1 in the transsynaptic control of vesicle accumulation. *Proc. Natl. Acad. Sci. USA* **107**, 11116–11121 (2010).
12. Hessler, N.A., Shirke, A.M. & Malinow, R. The probability of transmitter release at a mammalian central synapse. *Nature* **366**, 569–572 (1993).
13. Murthy, V.N., Sejnowski, T.J. & Stevens, C.F. Heterogeneous release properties of visualized individual hippocampal synapses. *Neuron* **18**, 599–612 (1997).
14. Rosenmund, C., Clements, J.D. & Westbrook, G.L. Nonuniform probability of glutamate release at a hippocampal synapse. *Science* **262**, 754–757 (1993).
15. Pang, Z.P. & Sudhof, T.C. Cell biology of Ca2+-triggered exocytosis. *Curr. Opin. Cell Biol.* **22**, 496–505 (2010).
16. Zucker, R.S. & Regehr, W.G. Short-term synaptic plasticity. *Annu. Rev. Physiol.* **64**, 355–405 (2002).
17. Branco, T., Staras, K., Darcy, K.J. & Goda, Y. Local dendritic activity sets release probability at hippocampal synapses. *Neuron* **59**, 475–485 (2008).
18. Frank, C.A., Kennedy, M.J., Goold, C.P., Marek, K.W. & Davis, G.W. Mechanisms underlying the rapid induction and sustained expression of synaptic homeostasis. *Neuron* **52**, 663–677 (2006).
19. Jakawich, S.K. *et al.* Local presynaptic activity gates homeostatic changes in presynaptic function driven by dendritic BDNF synthesis. *Neuron* **68**, 1143–1158 (2010).
20. Lindskog, M. *et al.* Postsynaptic GluA1 enables acute retrograde enhancement of presynaptic function to coordinate adaptation to synaptic inactivity. *Proc. Natl. Acad. Sci. USA* **107**, 21806–21811 (2010).
21. Frank, C.A., Pielage, J. & Davis, G.W. A presynaptic homeostatic signaling system composed of the Eph receptor, ephexin, Cdc42, and CaV2.1 calcium channels. *Neuron* **61**, 556–569 (2009).
22. Futai, K. *et al.* Retrograde modulation of presynaptic release probability through signaling mediated by PSD-95-neuroligin. *Nat. Neurosci.* **10**, 186–195 (2007).
23. Ryan, T.A., Reuter, H. & Smith, S.J. Optical detection of a quantal presynaptic membrane turnover. *Nature* **388**, 478–482 (1997).
24. Tokuoka, H. & Goda, Y. Activity-dependent coordination of presynaptic release probability and postsynaptic GluR2 abundance at single synapses. *Proc. Natl. Acad. Sci. USA* **105**, 14656–14661 (2008).
25. Takeichi, M. Cadherins: a molecular family important in selective cell-cell adhesion. *Annu. Rev. Biochem.* **59**, 237–252 (1990).
26. Brault, V. *et al.* Inactivation of the beta-catenin gene by Wnt1-Cre-mediated deletion results in dramatic brain malformation and failure of craniofacial development. *Development* **128**, 1253–1264 (2001).
27. Passafaro, M., Nakagawa, T., Sala, C. & Sheng, M. Induction of dendritic spines by an extracellular domain of AMPA receptor subunit GluR2. *Nature* **424**, 677–681 (2003).
28. Ripley, B., Otto, S., Tiglio, K., Williams, M.E. & Ghosh, A. Regulation of synaptic stability by AMPA receptor reverse signaling. *Proc. Natl. Acad. Sci. USA* **108**, 367–372 (2011).
29. Song, J.Y., Ichtchenko, K., Sudhof, T.C. & Brose, N. Neuroligin 1 is a postsynaptic cell-adhesion molecule of excitatory synapses. *Proc. Natl. Acad. Sci. USA* **96**, 1100–1105 (1999).
30. Burrone, J. & Murthy, V.N. Synaptic gain control and homeostasis. *Curr. Opin. Neurobiol.* **13**, 560–567 (2003).
31. Pozo, K. & Goda, Y. Unraveling mechanisms of homeostatic synaptic plasticity. *Neuron* **66**, 337–351 (2010).
32. Turrigiano, G.G. The self-tuning neuron: synaptic scaling of excitatory synapses. *Cell* **135**, 422–435 (2008).
33. Burrone, J., O'Byrne, M. & Murthy, V.N. Multiple forms of synaptic plasticity triggered by selective suppression of activity in individual neurons. *Nature* **420**, 414–418 (2002).
34. Han, E.B. & Stevens, C.F. Development regulates a switch between post- and presynaptic strengthening in response to activity deprivation. *Proc. Natl. Acad. Sci. USA* **106**, 10817–10822 (2009).
35. Nakayama, K., Kiyosue, K. & Taguchi, T. Diminished neuronal activity increases neuron-neuron connectivity underlying silent synapse formation and the rapid conversion of silent to functional synapses. *J. Neurosci.* **25**, 4040–4051 (2005).
36. Wierenga, C.J., Walsh, M.F. & Turrigiano, G.G. Temporal regulation of the expression locus of homeostatic plasticity. *J. Neurophysiol.* **96**, 2127–2133 (2006).
37. Bredt, D.S. & Nicoll, R.A. AMPA receptor trafficking at excitatory synapses. *Neuron* **40**, 361–379 (2003).
38. Newpher, T.M. & Ehlers, M.D. Glutamate receptor dynamics in dendritic microdomains. *Neuron* **58**, 472–497 (2008).
39. Sheng, M. & Hoogenraad, C.C. The postsynaptic architecture of excitatory synapses: a more quantitative view. *Annu. Rev. Biochem.* **76**, 823–847 (2007).
40. Sutton, M.A. & Schuman, E.M. Dendritic protein synthesis, synaptic plasticity, and memory. *Cell* **127**, 49–58 (2006).
41. Thiagarajan, T.C., Lindskog, M. & Tsien, R.W. Adaptation to synaptic inactivity in hippocampal neurons. *Neuron* **47**, 725–737 (2005).
42. Cingolani, L.A. *et al.* Activity-dependent regulation of synaptic AMPA receptor composition and abundance by beta3 integrins. *Neuron* **58**, 749–762 (2008).
43. Gainey, M.A., Hurvitz-Wolff, J.R., Lambo, M.E. & Turrigiano, G.G. Synaptic scaling requires the GluR2 subunit of the AMPA receptor. *J. Neurosci.* **29**, 6479–6489 (2009).
44. Wierenga, C.J., Ibata, K. & Turrigiano, G.G. Postsynaptic expression of homeostatic plasticity at neocortical synapses. *J. Neurosci.* **25**, 2895–2905 (2005).
45. Nuriya, M. & Huganir, R.L. Regulation of AMPA receptor trafficking by N-cadherin. *J. Neurochem.* **97**, 652–661 (2006).
46. Cathala, L., Holderith, N.B., Nusser, Z., DiGregorio, D.A. & Cull-Candy, S.G. Changes in synaptic structure underlie the developmental speeding of AMPA receptor-mediated EPSCs. *Nat. Neurosci.* **8**, 1310–1318 (2005).
47. Ryan, T.A. *et al.* The kinetics of SV recycling measured at single presynaptic boutons. *Neuron* **11**, 713–724 (1993).
48. Arikkath, J. & Reichardt, L.F. Cadherins and catenins at synapses: roles in synaptogenesis and synaptic plasticity. *Trends Neurosci.* **31**, 487–494 (2008).
49. Gottmann, K. Transsynaptic modulation of the synaptic vesicle cycle by cell-adhesion molecules. *J. Neurosci. Res.* **86**, 223–232 (2008).
50. Tanaka, H. *et al.* Molecular modification of N-cadherin in response to synaptic activity. *Neuron* **25**, 93–107 (2000).

© 2012 Nature America, Inc. All rights reserved.
npg

ONLINE METHODS

DNA constructs. The full-length N-cadherin, dominant-negative N-cadherin (DN-NCad), N-cadherin C-terminal deletion (NC-ΔC), β-catenin ΔPDZ, β-catenin ΔARM and Cre-pIRES2-EGFP constructs were as previously described[5]. A commercially available shRNA against N-cadherin and control (Mission shRNA; Sigma-Aldrich) was used in this study. GluA2 siRNA and control were kindly provided by M. Passafaro.

Neuronal cell cultures and transfection. Animal care and use protocols were approved by the UK Home Office. Dissociated hippocampal cultures were prepared from P0–P1 rats or β-catenin-floxed mice (provided by R. Kemler) and plated at low density onto an astrocyte feeder layer. The cultures were maintained as described previously[17]. Neurons were transfected at DIV 10 using a Ca^{2+} phosphate protocol[42]. β-catenin ΔPDZ, β-catenin ΔARM, NC shRNA and scrambled shRNA constructs were cotransfected with a GFP-expressing plasmid. Cultures were used for experiments at DIV 12–14. Where noted, cells were treated with TTX (1 μM) for 36 h before experiments.

Live labeling and immunocytochemistry. Anti-synaptotagmin1 uptake experiments were performed by delivering 900 action potentials to neurons by field stimulation in the presence of a rabbit polyclonal antibody to the luminal domain of synaptotagmin-1 (1:100, Synaptic Systems) diluted in normal HEPES-buffered bath solution (EBS) containing (in mM) 137 NaCl, 5 KCl, 2 $CaCl_2$, 2 $MgCl_2$, 10 D-glucose, 5 HEPES, 0.1 picrotoxin, 20 μM 6-cyano-7-nitroquinoxaline-2,3-dione (CNQX) and 50 μM D-2-amino-5-phosphonovaleric acid (AP5) at room temperature (23–26 °C). After two washes with normal EBS, the cells were fixed in 4% (wt/vol) paraformaldehyde in PBS. Surface labeling for GluA1 and GluA2 was carried out using rabbit polyclonal anti-GluA1 (1:10, Calbiochem) or mouse monoclonal anti-GluA2 (1:200, Chemicon) in culture medium for 15 min at 37 °C, followed by rinsing with EBS and fixation in 4% paraformaldehyde as above.

In all experiments, cells were permeabilized after fixation with 0.1% Triton X-100 and blocked in PBS containing 0.2 M glycine, 10% (vol/vol) FBS and 0.1% Triton X-100 for 1 h at room temperature. Primary antibodies were added in blocking solution and incubated for 2 h at room temperature. The following primary antibodies and dilutions were used: rabbit anti-GluA2/3 (1:250, Chemicon), mouse anti-bassoon (1:1,000, StressGen Biotech), rabbit anti-synapsin (1:2,000, Synaptic Systems), mouse anti-synapsin (1:1,000, Synaptic Systems), mouse anti-synaptophysin (1:500, Synaptic Systems), rabbit anti-synaptophysin (1:500, Synaptic Systems), chicken anti-GFP (1:1,000, Abcam), mouse anti–β-catenin (1:250, BD Biosciences), rabbit anti-Tau (1:800, Abcam), mouse anti-neurofilament H (1:500, Millipore), mouse anti-neuroligin (1:250, Synaptic System) and rabbit anti-vGlut1 (1:2,000, Synaptic Systems). After three washes in PBS, neurons were incubated with secondary fluorescently conjugated antibodies (Alexa Fluor 568 (Invitrogen), Cy2 or Cy5 (Jackson Laboratories)).

Correlative transmission electron microscopy. After identifying transfected cells, fluorescence and brightfield images of the regions of interest were acquired at different magnifications using an Olympus BX50WI upright epifluorescence microscope. Cells were fixed in 2% (wt/vol) paraformaldehyde, 2% (wt/vol) glutaraldehyde (both EM grade from TAAB) in 0.1 M sodium cacodylate buffer for 30 min at room temperature. Samples were then secondarily fixed in 1% (wt/vol) osmium tetroxide, 1.5% (wt/vol) potassium ferricyanide for 1 h at 4 °C. After washes in 0.1 M sodium cacodylate, coverslips were incubated in 1% (wt/vol) tannic acid in 0.5 M sodium cacodylate at room temperature for 45 min. Further washes in 0.5 M sodium cacodylate were followed by a final wash in distilled water, before the samples underwent dehydration by sequential short incubations in 70% (vol/vol) and 90% (vol/vol) ethanol and then two longer incubations in 100% ethanol. Coverslips were transferred to a 1:1 mix of propylene oxide and Epon resin (TAAB) for 90 min, then 100% Epon for two more 90-min incubations. Finally coverslips were inverted onto prepolymerized Epon stubs, ensuring that the area of interest was safely on the stub itself, and samples were polymerized by baking at 60 °C overnight. Coverslips were removed by rapid immersion of the samples in liquid nitrogen. The cells of interest were found on the block surface using the light microscopy images. Small block faces were trimmed and then serial, 70-nm ultrathin sections cut with a diamond knife. Ribbons of sections were collected on polyvinyl formal (Formvar)-coated 2 mm × 1 mm slot grids and stained using Reynolds lead citrate before imaging. Samples were imaged using an FEI Tecnai G2 Spirit transmission electron microscope and an Olympus SIS Morada CCD camera. Asymmetric (excitatory) synapses were identified by a thick postsynaptic density and presence of round vesicles in presynaptic terminals. Per single section, the total number of synaptic vesicles and the number of docked vesicles in direct contact with the presynaptic terminal at the active zone defined by the postsynaptic apposition to the postsynaptic density were counted.

FM imaging. Epifluorescence images were acquired on an Olympus BX50WI upright microscope using a cooled CCD camera (Princeton Instruments). Synaptic vesicles were labeled by 7, 40 or 900 action potentials delivered by field stimulation in a custom-made chamber in the presence of FM4-64 (15 μM, Invitrogen); 45 s after the end of stimulation the excess dye was washed with EBS containing 1 mM Advasep-7 (Biotium) for 1 min and then rinsed with EBS for 10 min. Images were acquired every 30 s before and after unloading stimulation by 600 action potentials at 20 Hz for three rounds with 15-s intervals or 900 action potentials at 10 Hz. The remaining signal was taken as background. Experiments were carried out in normal EBS except for experiments monitoring extracellular Ca^{2+} sensitivity (**Fig. 4c**), where the FM dye loading was performed in EBS containing 2 or 5 mM Ca^{2+}. FM4-64 dye destaining kinetics was monitored during unloading stimulation of 600 action potentials at 2 Hz. In pulse-chase FM4-64 experiments, the cultures were stimulated by 300 action potentials at 10 Hz and exposed to the dye for 1 min after a variable delay time from the end of stimulation. All experiments were performed at room temperature.

Image analysis. Transfected neurons were quantified from at least two independent experiments for each construct. The number of neurons or puncta used for quantification is indicated in the figures. Images were analyzed using MetaMorph imaging software (Universal Imaging Corporation). To quantify signals associated with pre- and postsynaptic markers, background signal (nonpunctate region) was subtracted and integrated fluorescence intensity of individual puncta was measured and averaged per neuron, and the ratio between values in transfected cells and those in untransfected neurons in the same coverslip was determined. The number of neurons from which the ratio of mean values was averaged to calculate the population mean is indicated in figure legends. For measurements of total synaptic GluA2/3 and surface synaptic GluA1 and GluA2, we restricted our analysis to synapses that showed partially or completely overlapping signals between postsynaptic receptors and presynaptic markers.

To quantify FM4-64 fluorescence, background signals were subtracted, and integrated fluorescence intensities of individual puncta were measured using MetaMorph. Release probability was estimated by optical quantal analysis as previously described with slight modifications[24]. FM4-64 was loaded by 40 action potentials at 1 Hz and p_r was $(F/q)/40$, where F is the integrated fluorescence intensity of the FM4-64 puncta and q is the quantal FM4-64 fluorescence measured from sister coverslips on the same day (in which FM was loaded by 7 action potentials at 0.5 Hz)[13,23,24]. Release probability was calculated for each synapse and averaged per neuron.

Electrophysiology. Whole cell patch-clamp recordings were carried out in a culture chamber placed on the stage of an Olympus IX70 inverted microscope at room temperature and using Axopatch 200B or multiclamp amplifiers (Axon Instruments). Transfected cells were identified using standard epifluorescence. The recording chamber was continuously perfused with an artificial cerebrospinal fluid containing (in mM) 130 NaCl, 2.5 KCl, 2.2 $CaCl_2$, 1.5 $MgCl_2$, 10 D-glucose, 10 HEPES, 0.1 picrotoxin, pH 7.35, adjusted to 290 mOsm. TTX (0.5 μM) was added to block sodium channels when recording mEPSCs. The intracellular solution contained (in mM) 100 potassium gluconate, 17 KCl, 5 NaCl, 5 $MgCl_2$, 10 HEPES, 0.5 EGTA, 4 K_2-ATP, 0.5 Na-GTP, pH 7.3, adjusted to 280 mOsm. Recorded neurons were held under voltage clamp at −70 mV and series resistance was left uncompensated. Pipette resistance was 3–5 MΩ, and only cells with a stable resting potential of <−50 mV and series resistance of <20 MΩ were analyzed.

For paired recordings, monosynaptic connections were identified by a short latency (<10 ms). Short-term plasticity was monitored by evoking ten action

© 2012 Nature America, Inc. All rights reserved.

doi:10.1038/nn.2995

potentials at 25 Hz with brief depolarizations (1 ms, 100 mV) of the presynaptic neuron. The amplitude of the evoked postsynaptic responses was measured using Clampfit software (Axon Instruments).

mEPSCs were recorded over a period of 5–10 min, and recordings were filtered at 2 kHz and sampled at 10 kHz using pClamp software (Axon Instruments). Amplitude, frequency and decay time (90–37% of the peak amplitude) of the events were analyzed using mini analysis software (Synaptosoft). The detection threshold was set at –6 pA. Cells with a noisy or unstable baseline were discarded. Raw data were inspected to eliminate any false events.

Statistics. Statistical significance was determined by the two-tailed Student's *t* test or one-way ANOVA. The Mann-Whitney test was used when criteria for normality were not met. All data are shown as the mean ± s.e.m. Statistical significance was assumed when $P < 0.05$. In figures, $^{*}P < 0.05$, $^{**}P < 0.01$ and $^{***}P < 0.001$.

© 2012 Nature America, Inc. All rights reserved.